RESEARCH ARTICLE

Key Points:
- *Trichodesmium* fixes nitrogen in surface waters at 160°E–170°W
- Subsurface water east of 90°W affected by in situ water column denitrification
- δ^{15}N–NO$_3^-$ values reflect water circulation as well as biological processes

Correspondence to:
C. Yoshikawa,
yoshikawac@jamstec.go.jp

Nitrogen isotope ratios of nitrate and N* anomalies in the subtropical South Pacific

Chisato Yoshikawa[1], Akiko Makabe[2], Takuhei Shiozaki[3], Sakae Toyoda[4], Osamu Yoshida[5], Ken Furuya[3], and Naohiro Yoshida[4,6]

[1]Department of Biogeochemistry, Japan Agency for Marine-Earth Science and Technology, Yokosuka, Japan, [2]Graduate School of Agriculture, Tokyo University of Agriculture and Technology, Tokyo, Japan, [3]Graduate School of Agricultural and Life Sciences, University of Tokyo, Tokyo, Japan, [4]Interdisciplinary Graduate School of Science and Engineering, Tokyo Institute of Technology, Yokohama, Japan, [5]Department of Environmental and Symbiotic Science, College of Agriculture, Food and Environment Sciences, Rakuno Gakuen University, Ebetsu, Japan, [6]Earth-Life Science Institute, Tokyo Institute of Technology, Tokyo, Japan

Abstract Nitrogen isotopic ratios of nitrate (δ^{15}N–NO$_3^-$) were analyzed above 1000 m water depth along 17°S in the subtropical South Pacific during the revisit WOCE P21 cruise in 2009. The δ^{15}N–NO$_3^-$ and N* values were as high as 17‰ and as low as -18 μmol N L^{-1}, respectively, at depths around 250 m east of 115°W, but were as low as 5‰ and as high as $+1$ μmol N L^{-1}, respectively, in subsurface waters west of 170°W. The relationships among NO$_3^-$ concentrations, N* values, δ^{15}N–NO$_3^-$ values, and oxygen and nitrite concentrations suggest that a few samples east of 90°W were from suboxic and nitrite-accumulated conditions and were possibly affected by in situ water column denitrification. Most of the high-δ^{15}N–NO$_3^-$ and negative-N* waters were probably generated by mixing between Subantarctic Mode Water from the Southern Ocean and Oxygen Deficit Zone Water from the eastern tropical South Pacific, with remineralization of organic matter occurring during transportation. Moreover, the relationship between δ^{15}N–NO$_3^-$ and N* values, as well as *Trichodesmium* abundances and size-specific nitrogen fixation rates at the surface, suggest that the low-δ^{15}N–NO$_3^-$ and positive-N* subsurface waters between 160°E and 170°W were generated by the input of remineralized particles created by in situ nitrogen fixation, mainly by *Trichodesmium* spp. Therefore, the δ^{15}N values of sediments in this region are expected to reveal past changes in nitrogen fixation or denitrification rates in the subtropical South Pacific.

1. Introduction

The nitrogen (N) cycle in the subtropical South Pacific exhibits distinct east-west differences. *Deutsch et al.* [2001] reported a N deficit compared with phosphorus (P) in the east and a N excess in the west, based on nutrient data collected during the World Ocean Circulation Experiment (WOCE P21) cruise along 17°S in 1994. They used a quasi-conservative tracer, N*, defined as N* = (NO$_3^-$ $-$ 16PO$_4^{3-}$ $+$ 2.9) $\times$ 0.87 [*Gruber and Sarmiento*, 1997]. Although biogeochemical cycling in Redfield proportions [*Redfield et al.*, 1963] does not generate N* anomalies, external N inputs (N fixation and atmospheric N deposition) and N outputs (denitrification) with non-Redfield elemental cycling can generate N* anomalies. Furthermore, N fixation commonly occurs in oligotrophic regions, when N fixers take up dinitrogen (N$_2$) gas instead of nitrogenous nutrients. When this occurs, N* increases due to the addition of N in the absence of a commensurate addition of P. Similarly, atmospheric N deposition out of Redfield proportions can alter N*. In contrast, denitrification occurs in low-oxygen waters because NO$_3^-$ is used instead of oxygen in bacterial respiration. This denitrification decreases N* because NO$_3^-$ is consumed in the absence of a commensurate loss of P. N* can therefore be used to trace water masses affected by N fixation/deposition and denitrification. However, the N* field may also be affected by mixing of waters with nonzero N* values or by non-Redfield assimilation and remineralization [e.g., *Clark et al.*, 1998; *Yoshikawa et al.*, 2013; *Martiny et al.*, 2013]. Therefore, complementary tracers are necessary to elucidate the N cycle precisely.

Nitrogen isotopic ratios of nitrate (δ^{15}N–NO$_3^-$) are also widely used as a tracer of external N inputs and outputs. N fixation produces fixed N with a δ^{15}N value of $\sim$0‰, as N fixers take up N$_2$ gas (δ^{15}N = 0‰) with little isotopic effect [e.g., *Minagawa and Wada*, 1986]. This fixed N with low δ^{15}N values ($\sim$0‰) is eventually
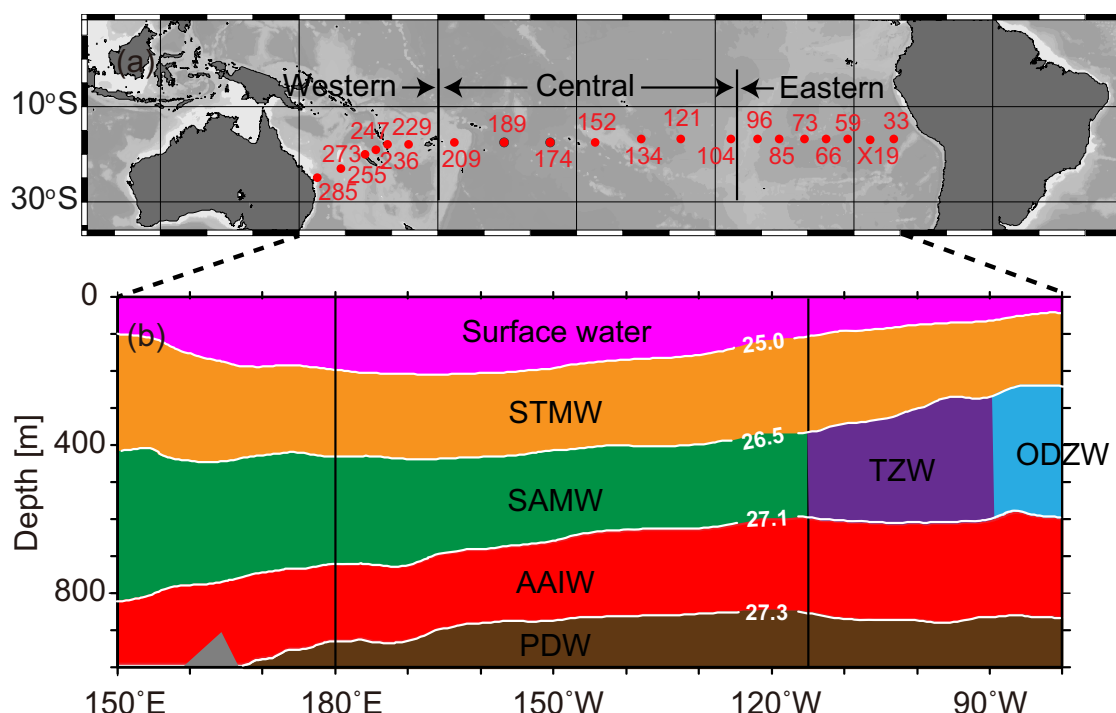
Figure 1. Map of the subtropical South Pacific showing (a) locations of hydrocast stations during the MR09-01 cruise, and (b) horizontal distributions of potential density (kg m^{-3}) with water mass names: Surface water, Subtropical Mode Water (STMW), Subantarctic Mode Water (SAMW), Oxygen Deficit Zone Water (ODZW), Transition Zone Water (TZW), Antarctic Intermediate Water (AAIW), and Pacific Deep Water (PDW).

converted into low δ^{15}N–NO$_3^-$ through remineralization. The δ^{15}N values of atmospheric NO$_3^-$ ($-46.9‰$ to $+14.1‰$) are lower than those of marine NO$_3^-$ (deep water δ^{15}N–NO$_3^-$ = approx. $+5‰$, reported by *Sigman et al.* [2009]) [e.g., *Elliott et al.*, 2009; *Savarino et al.*, 2007]. Atmospheric N inputs and river discharge therefore decrease the δ^{15}N–NO$_3^-$ values of ambient NO$_3^-$. When denitrification occurs in the water column, δ^{15}N–NO$_3^-$ values increase due to a strong isotopic effect of $+10$ to $+30‰$ [e.g., *Barford et al.*, 1999; *Granger et al.*, 2008; *De Pol-Holz et al.*, 2009; *Kritee et al.*, 2012].

Rafter et al. [2012] measured δ^{15}N–NO$_3^-$ and N* values in the tropical Pacific. They discussed the transformation of these tracer signals during transportation from the eastern subarctic South Pacific to the tropical Pacific, using their data together with previously reported data obtained for the South Pacific [*De Pol-Holz et al.*, 2009; *Liu*, 1979; *Sigman et al.*, 2000]. Although the subtropical South Pacific is located in the direct path of this transportation, the δ^{15}N–NO$_3^-$ values in this region have only been measured once, along a north-south transect in the South Pacific region [*Rafter et al.*, 2013].

To ascertain how the eastern N deficit and western N excess in the subtropical South Pacific is generated and how the δ^{15}N–NO$_3^-$ and N* signals in the South Pacific are propagated, we analyzed δ^{15}N–NO$_3^-$ and N* values during the revisit WOCE P21 cruise in 2009.

2. Materials and Methods

Water sampling and conductivity, temperature, and depth (CTD) observations were conducted along 17°S during cruise MR09-01 of the R/V *Mirai*, Japan Agency for Marine-Earth Science and Technology (JAMSTEC), during April–June 2009. Water samples for NO$_3^-$ isotopic analysis were collected from 20 profiles, ranging from water depths of 0–1000 m, using rosette-mounted Niskin bottles (Figure 1a). They were filtered immediately after sampling. These samples were then preserved at $-20°$C until chemical analysis. Water samples for N fixation rates and *Trichodesmium* abundance were collected from the surface with a bucket at stations every 2–5°. Additionally, water samples for *Trichodesmium* abundance were collected from 4.5 m depth by using the underway water supply for research at stations every ~2°. Samples for N fixation rates were
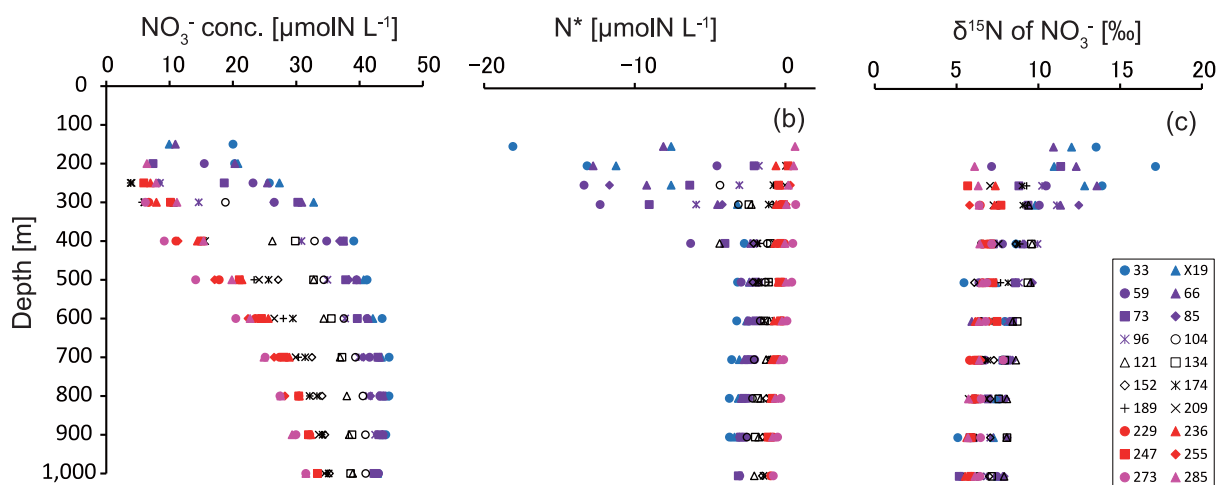
Figure 2. Vertical distributions of (a) NO_3^- concentrations (μmol N L^{-1}), (b) N* values (μmol N L^{-1}), and (c) δ^{15}N–NO_3^- values (‰) in the subtropical South Pacific.

injected with ^{15}N$_2$ gas and incubated in an on-deck incubator, although the N fixation rates in this method could be underestimated compared with those estimated by the N$_2$ dissolution method [*Mohr et al.*, 2010; *Großkopf et al.*, 2012]. Samples collected for measuring *Trichodesmium* abundance were fixed with acidified Lugol's solution and enumerated by the Utermöhl method using an inverted microscope. The N fixation rates and *Trichodesmium* abundances are both from the data set published by *Shiozaki et al.* [2014]. The sampling, analyses, and calculations for N fixation rates and *Trichodesmium* abundances are described in detail in *Shiozaki et al.* [2014]. The data and analytical procedures for water temperature, salinity, dissolved oxygen, and nutrient concentrations are available from the *Mirai* database (http://www.godac.jamstec.go.jp/cruisedata/mirai/e/index.html).

The δ^{15}N values of NO_3^- (plus nitrite) in seawater samples, of which the NO_3^- concentrations are more than 1 μmol N L^{-1}, were measured using the bacterial method of *Sigman et al.* [2001]. Briefly, NO_3^- was converted to N$_2$O by denitrifying bacteria that lack N$_2$O-reductase activity. The N$_2$O produced was then analyzed using a ThermoFinnigan GasBench + PreCon trace gas concentration system interfaced to a ThermoScientific Delta V Plus isotope-ratio mass spectrometer at the University of California, Davis, Stable Isotope Facility (http://stableisotopefacility.ucdavis.edu/). The calibration standards used were USGS 32, USGS 34, and USGS 35. The precision for these analyses was $\pm$0.2‰ for δ^{15}N. The presence of nitrite can result in underestimation of the δ^{15}N–NO_3^- value when using the bacterial method [*Casciotti and McIlvin*, 2007]. Therefore, we show here only the δ^{15}N–NO_3^- values of samples with a nitrite concentration of less than 0.03 μmol N L^{-1} and a nitrite percentage of the nitrate concentration of less than 0.3%

3. Results and Discussion

3.1. δ^{15}N–NO_3^- and N* Values

Figures 2 and 3 show the vertical and longitudinal distributions, respectively, of NO_3^- concentrations, δ^{15}N–NO_3^- values, and N* values in the subtropical South Pacific. The NO_3^- concentrations exhibit distinct east-west differences (Figures 2a and 3a); concentrations are higher in the eastern area compared with the western area due to the coastal upwelling off Peru. δ^{15}N–NO_3^- values are expected to increase toward the surface, in conjunction with NO_3^- depletion, due to the preferential uptake of ^{14}N–NO_3^- by phytoplankton [e.g., *Miyake and Wada*, 1971]. In addition, if nutrient uptake by phytoplankton and remineralization occur within Redfield proportions, and if external N inputs/output do not occur, then N* values should be ~0 μmol N L^{-1} [e.g., *Gruber and Sarmiento*, 1997]. However, in the subsurface waters of the eastern area, the δ^{15}N–NO_3^- values are as high as 17‰ (Figure 2c) and the N* values are as low as −18 μmol N L^{-1} (Figure 2b). In contrast, the δ^{15}N–NO_3^- values decrease and the N* values increase toward the surface in the western area (Figures 2b, 2c, 3b, and 3c).
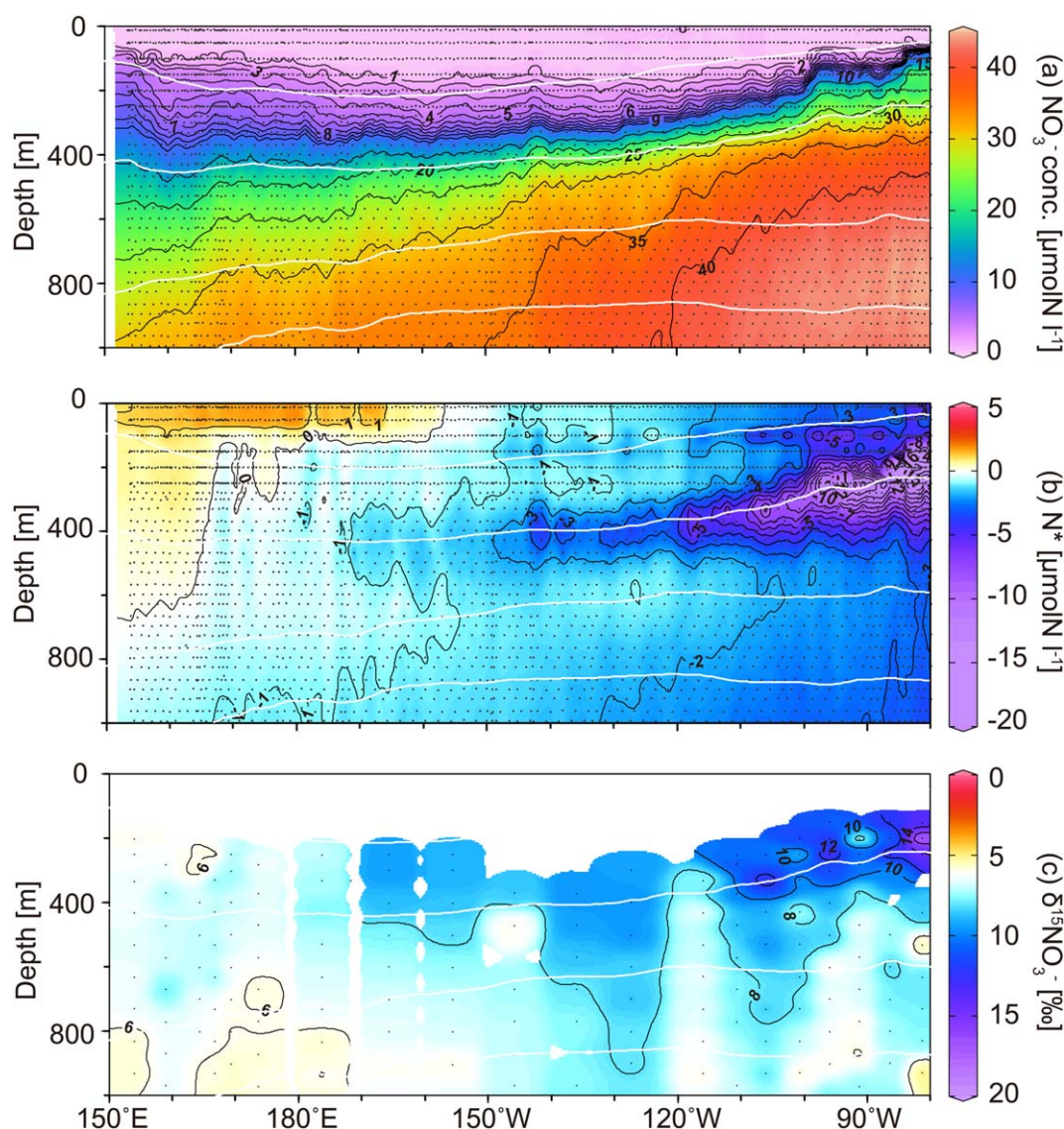
Figure 3. Longitudinal distributions of (a) nitrate concentrations (μmol N L^{-1}), (b) N* values (μmol N L^{-1}), and (c) δ^{15}N–NO$_3^-$ values (‰) along 17°S. Black dots indicate sampling points. White lines represent isopycnal surfaces. The surface cutoff in c is due to an insufficient concentration of nitrate or the presence of nitrite.

3.2. Physical Features

The samples were separated into five water types according to the density-based classification used by *Rafter et al.* [2012] (Figure 1b). By increasing depth, they are: Surface water (potential density (σ_θ) < 25.0), Subtropical Mode Water (STMW; σ_θ = 25.0–26.5), Subantarctic Mode Water (SAMW; σ_θ = 26.5–27.1), Antarctic Intermediate Water (AAIW; σ_θ = 27.1–27.3), and Pacific Deep Water (PDW; σ_θ > 27.3). In addition to this, SAMW east of 90°W was characterized as Oxygen Deficit Zone Water (ODZW), in which water column denitrification is known to occur [*De Pol-Holz et al.*, 2009]. SAMW between 115° and 90°W was characterized as Transition Zone Water (TZW), which forms from mixing between SAMW and ODZW [*Johnson and McTaggart*, 2010]. The studied stations were categorized into three areas: eastern, central, and western (Figure 1a). Stations to the east of 115°W, which encompassed areas of ODZW and the TZW, were categorized as eastern stations (stations 33–96). Stations to the west of 180°E, along the Australian coast and within archipelagic deep basin provinces, were categorized as western stations (stations 229–285). The remaining stations between 115°W and 180°E were categorized as central stations (stations 104–209). Table 1 presents the averaged values of physical and biogeochemical parameters for each water mass.

Table 1. Average Values of Select Parameters for Water Masses in the Subtropical South Pacific Along 17°S

Water Mass[a] (Density Range)	Nitrate (µM)		δ^{15}N of Nitrate (‰)		N* (µM)		Theta (°C)		Salinity		Dissolved Oxygen (µmol/kg)		Sigma Theta (kg/m³)	
E-STMW (25.0–26.5)	13.9	(7.2)[b]	10.5	(3.4)	−6.0	(4.9)	14.4	(2.4)	34.83	(0.28)	133.2	(71.2)	25.95	(0.33)
C-STMW (25.0–26.5)	9.8	(8.1)	6.8	(3.2)	−1.5	(1.0)	16.9	(3.8)	35.31	(0.48)	172.9	(14.9)	25.67	(0.43)
W-STMW (25.0–26.5)	7.4	(2.8)	6.3	(0.7)	0.2	(0.4)	17.4	(2.2)	35.46	(0.20)	176.5	(9.7)	25.76	(0.39)
ODZW (26.0–27.1)	34.5	(6.9)	9.7	(3.2)	−7.0	(4.5)	9.2	(1.8)	34.63	(0.08)	16.8	(13.4)	26.79	(0.23)
TZW (26.0–27.1)	35.4	(4.8)	8.8	(1.7)	−5.0	(3.5)	8.6	(1.6)	34.57	(0.07)	36.1	(26.4)	26.85	(0.20)
C-SAMW (26.5–27.1)	28.7	(5.6)	7.9	(1.1)	−1.5	(1.1)	7.8	(1.6)	34.48	(0.11)	142.9	(33.7)	26.88	(0.17)
W-SAMW (26.5–27.1)	22.3	(4.5)	6.6	(0.5)	−0.2	(0.3)	8.4	(2.1)	34.60	(0.20)	193.7	(7.1)	26.88	(0.18)
E-AAIW (27.1–27.3)	42.6	(1.5)	7.5	(0.8)	−2.5	(0.5)	5.6	(0.5)	34.50	(0.01)	52.4	(15.6)	27.21	(0.06)
C-AAIW (27.1–27.3)	34.9	(3.4)	7.0	(0.8)	−1.3	(0.4)	5.2	(0.4)	34.44	(0.04)	137.6	(33.2)	27.20	(0.06)
W-AAIW (27.1–27.3)	30.3	(1.6)	6.0	(0.3)	−0.7	(0.2)	5.2	(0.5)	34.42	(0.02)	182.1	(9.2)	27.19	(0.06)
E-PDW (>27.3)	43.0	(0.6)	6.6	(1.1)	−3.1	(0.3)	4.5	(0.3)	34.52	(0.01)	60.8	(7.8)	27.36	(0.04)
C-PDW (>27.3)	36.6	(2.8)	6.6	(0.8)	−1.6	(0.5)	4.2	(0.3)	34.48	(0.03)	130.2	(30.9)	27.37	(0.04)
W-PDW (>27.3)[c]	32.6	(1.0)	6.0	(0.3)	−1.0	(0.1)	4.3	(0.3)	34.46	(0.01)	168.4	(5.4)	27.33	(0.04)

[a]See Figure 1 for the names of water masses. "E," "C," and "W" are abbreviations for eastern, central, and western, respectively.
[b]Values in parentheses are standard deviations.
[c]The PDW values are averaged for measurements above the depth of 1000 m.

3.3. Nitrogenous Nutrient Inputs and Losses

To understand how the distinctive δ^{15}N–NO$_3^-$ and N* signals in the subtropical South Pacific are generated, Figure 4 exhibits the longitudinal distributions of surface size-specific N fixation rates and surface *Trichodesmium* abundances modified from *Shiozaki et al.* [2014], as well as oxygen and nitrite concentrations.

In subsurface waters of the eastern area, the N* values were negative (−6.0 ± 4.9 µmol N L^{-1} in E-STMW, −7.0 ± 4.5 µmol N L^{-1} in ODZW and −5.0 ± 3.5 µmol N L^{-1} in TZW) and the δ^{15}N–NO$_3^-$ values were high (10.5 ± 3.4‰ in E-STMW, 9.7 ± 3.2‰ in ODZW and 8.8 ± 1.7‰ in TZW) compared with the surrounding waters (see Table 1 and Figures 3b and 3c). The negative N* and high δ^{15}N–NO$_3^-$ values were associated with low-oxygen concentrations compared with the water masses in the central and western areas (Figure 4c). Moreover, the nitrite concentrations showed subsurface maxima created by surface biological production ($\sigma_\theta = 25.0$) and additional maxima ($\sigma_\theta = 26.5$) below (Figure 4d). These features indicated that the subsurface waters of the eastern area can be affected by denitrification. Water column denitrification occurs under oxygen concentrations of less than ~15 µmol kg^{-1} [e.g., *Pierotti and Rasmussen*, 1980]. Only 10 samples east of 100°W were suboxic with oxygen concentrations less than ~15 µmol kg^{-1}. They were found at depths of 200, 250, and 400 m at station 33, at 250 and 300 m at station X19, at 300 and 400 m at station 59, and at 250, 300, and 400 m at station 66. Moreover, water column denitrification creates a secondary nitrite maximum [e.g., *Naqvi et al.*, 2008]. Nitrite accumulated at depth around 300 m east of 90°W (Figure 4d). However, only 1 of 10 samples was from the secondary nitrite maximum; it was sampled at a depth of 300 m at station X19, and had a nitrite value of 0.02 µM. The nitrite concentration at 300 m depth at station 33 was 0.34 µM, but the δ^{15}N–NO$_3^-$ value cannot be shown here due to the effects of nitrite contamination of the nitrate pool on the δ^{15}N–NO$_3^-$ analysis. Apparently, in the other negative N* and high-δ^{15}N–NO$_3^-$ waters, water column denitrification did not occur in situ during a period of sampling, as oxygen values were too high. The waters must have been mixed with waters affected by denitrification occurring at other times and locations.

In subsurface waters of the western area, the N* values were positive (+0.2 ± 0.4 µmol N L^{-1} in W-STMW) and the δ^{15}N–NO$_3^-$ values were lower (6.3 ± 0.7‰ in W-STMW) than the values below W-STMW (6.6 ± 0.5‰ in W-SAMW) (see Table 1 and Figures 3b and 3c). In the surface waters between 160°E and 170°W, N fixation rates by N fixers, whose size exceeded 10 µm, were high, with rates up to 8 nmol N L^{-1} d^{-1} (Figure 4a). In addition, the abundance of *Trichodesmium* was high, with concentrations up to 1164 filaments L^{-1} (Figure 4b). In comparison, the abundance of the other microsize diazotroph, *Richelia intracellularis*, a symbiont of *Rhizosolenia clevei*, was ~1/100th that of *Trichodesmium* spp. [see *Shiozaki et al.*, 2014, Figure S2a]. The areas with high N fixation rates and high abundances of *Trichodesmium* at the surface were consistent with the areas of positive N* and low δ^{15}N–NO$_3^-$ values in the subsurface water (Figures 3b and 3c). However, the sampling depths of active N fixation and abundant *Trichodesmium* spp. were different from those of the low δ^{15}N–NO$_3^-$ values, because we were unable to collect surface δ^{15}N–NO$_3^-$ data due to insufficient
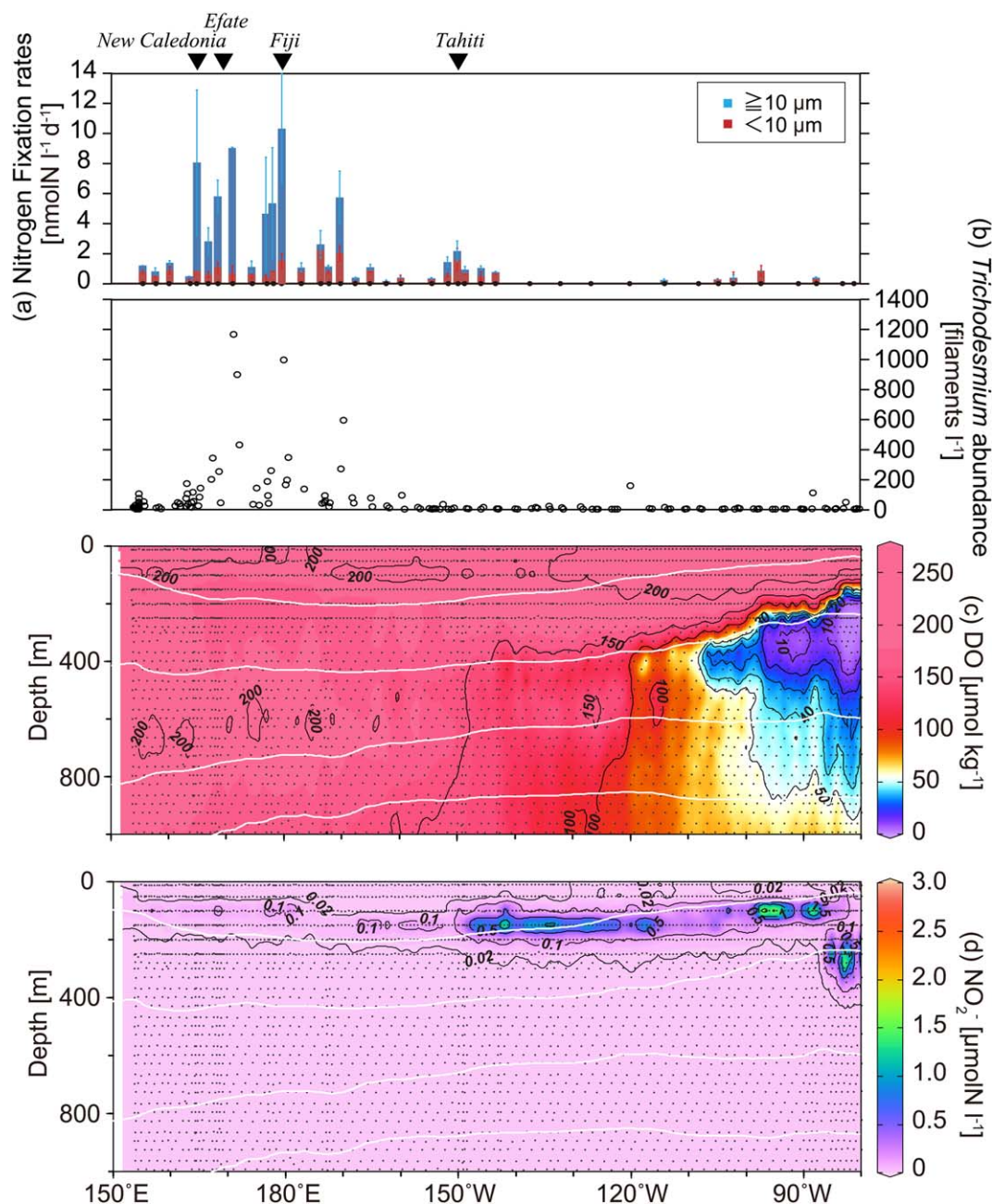
Figure 4. Longitudinal distributions of (a) size-specific surface nitrogen fixation rates (nmol N L^{-1} d^{-1}) and (b) surface abundances of *Trichodesmium* (filaments L^{-1}) modified from *Shiozaki et al*. [2014], as well as (c) oxygen concentrations (μmol kg^{-1}) and (d) nitrite concentrations (μmol N L^{-1}) along 17°S. Black dots indicate sampling points. White lines represent isopycnal surfaces.

concentrations of NO_3^- or the presence of NO_2^-. These facts suggest that the input of remineralized low-δ^{15}N particles created by N fixation and PO_4^- consumption in the absence of commensurate NO_3^- consumption by N_2 fixers (mainly *Trichodesmium*) cause low δ^{15}N values and excess N in W-STMW water east of 160°E. In the waters west of 160°E, both the abundance of *Trichodesmium* and the N fixation rates were much lower than in water east of 160°E (Figures 4a and 4b). However, in the waters west of 160°E, the δ^{15}N–NO_3^- values were low and the N* values were high throughout the water column compared with corresponding depths in the water east of 160°E (pink symbols in Figures 2b, 2c, 3b, and 3c). As *Trichodesmium* blooms are episodic but N* and δ^{15}N–NO_3^- values become integrated over long time periods, the water west of 160°E could be affected not only by in situ N fixation during a period of sampling but also by N fixation at other times and locations, as well as by atmospheric deposition or river discharge.

3.4. Propagation of the δ^{15}N–NO$_3^-$ and N* Signals in the South Pacific

Rafter et al. [2012] found low δ^{15}N–NO$_3^-$ values in the Southern Subsurface Counter Current (SSCC) (5.5 ± 0.3‰). They reported that the low δ^{15}N–NO$_3^-$ is derived from remineralized products of N fixation in the northern Tasman Sea, Coral Sea, and/or South Pacific gyre. Because the western area of this study is located in the Coral Sea and the northern Tasman Sea, the low δ^{15}N–NO$_3^-$ in W-STMW (6.3 ± 0.7‰) must be one origin of the low δ^{15}N–NO$_3^-$ in the SSCC. However, the NO$_3^-$ concentrations in W-STMW are much lower than those in the SSCC (7.4 ± 2.8 μmol N L^{-1} in W-STMW compared with 25.7 ± 8.9 μmol N L^{-1} in the SSCC) (Figure 5a). Moreover, although the SSCC might be affected by mixing between W-STMW with low NO$_3^-$ concentrations (7.4 ± 2.8 μmol N L^{-1}) and deeper water with high NO$_3^-$ concentrations (22.3 ± 4.5 μmol N L^{-1} in W-SAMW), the δ^{15}N–NO$_3^-$ values in the western subsurface waters (6.6 ± 0.5‰ in W-SAMW) are much higher than those in the SSCC (5.5 ± 0.3‰ in SSCC) (Figure 5a). Therefore, we infer that the SSCC is affected by further addition of low δ^{15}N–NO$_3^-$ during transportation from the western subtropical South Pacific to the equatorial Pacific.

The ODZW and TZW are derived from SAMW in the Pacific sector of the Southern Ocean (SO SAMW), with ODZW originating in the eastern tropical South Pacific (ETSP ODZW). Both ODZW and TZW are then transported to the equatorial Pacific (Eq. Pacific SAMW) [see *Rafter et al.*, 2012, Figures 1b and 1c]. If denitrification and remineralization do not affect ODZW, TZW, and Eq. Pacific SAMW, then the relationships between NO$_3^-$ concentrations, N* values, and δ^{15}N–NO$_3^-$ values in the ODZW, TZW, and Eq. Pacific SAMW are expected to lie on the mixing lines between SO SAMW and ETSP ODZW (gray lines in Figures 5c and 5d). The relationship between the δ^{15}N–NO$_3^-$ and N* values lies on the mixing line (Figure 5d), but that between the δ^{15}N–NO$_3^-$ values and NO$_3^-$ concentrations does not (Figure 5c). ODZW, TZW, and Eq. Pacific SAMW have much higher NO$_3^-$ concentrations than the inferred mixture between SO SAMW and ETSP ODZW. *Rafter et al.* [2012] explained that the reason for such high NO$_3^-$ concentrations in the Eq. Pacific SAMW is the addition of NO$_3^-$ through remineralization of organic matter. ODZW and TZW must also be affected by remineralization.

In addition to the mixing of water between SO SAMW and ETSP ODZW, there are two groupings of values that show organic matter is remineralized to NO$_3^-$ (Figures 5c and 5d); one with remineralization occurring at N* = 0 and δ^{15}N–NO$_3^-$ = 6.3‰ (red shaded area in the figure) and one with remineralization occurring at N* = 0 and δ^{15}N–NO$_3^-$ = 12.0‰ (blue shaded area). We assumed that the NO$_3^-$ concentrations produced by remineralization are between 6 and 20 μmol N L^{-1}, which are the minimum and maximum differences in NO$_3^-$ concentrations between the mixing line and ODZW, TZW, and Eq. Pacific SAMW. Samples of Eq. Pacific SAMW are shown within the red shaded area in Figures 5c and 5d. Most of the samples of ODZW and TZW are shown within the blue shaded area in Figures 5c and 5d; some samples from suboxic conditions (black dots in Figures 5c and 5d) are shown above the shaded areas because a large isotopic fractionation occurs during water column denitrification [e.g., *Barford et al.*, 1999; *Granger et al.*, 2008; *De Pol-Holz et al.*, 2009; *Kritee et al.*, 2012]. Moreover, some samples obtained from around 500 m depth at stations 33, 59, and 66 are shown below the shaded areas. The surface N fixation rates and *Trichodesmium* abundances show small peaks (Figures 4a and 4b). Therefore, the low δ^{15}N–NO$_3^-$ with low N* values are possibly a result of remineralization of organic matter affected by N fixation at stations 33, 59, and 66. *Rafter et al.* [2013] suggested that partial nitrate assimilation in the surface of the Southern Ocean leads to the introduction of low δ^{15}N–NO$_3^-$ through organic matter remineralization. Therefore, the low-δ^{15}N–NO$_3^-$ and low-N* water are possibly a result of the remineralization of relatively low-δ^{15}N organic matter in the Southern Ocean. From these results, we infer that the δ^{15}N–NO$_3^-$ and N* signals of SO SAMW mix with those of ETSP ODZW, and as the water is transported to the eastern subtropical South Pacific these signals are also influenced by remineralized organic matter. The SAMW in the eastern subtropical South Pacific is further mixed and affected by remineralization during transport to the equatorial Pacific thermocline via the South Pacific gyre circulation and the equatorial undercurrent. Moreover, the δ^{15}N–NO$_3^-$ and N* signals in ODZW and TZW could be affected by both denitrification and N fixation in the subtropical South Pacific or by remineralization in the Southern Ocean.

The relationship between NO$_3^-$ concentrations and N* and δ^{15}N–NO$_3^-$ values in the western deeper waters (W-AAIW and W-PDW) resembles that of SO AAIW (Figures 5e and 5f). The eastern deeper waters have much higher NO$_3^-$ concentrations and δ^{15}N–NO$_3^-$ values, and much lower N* values (42.6 ± 1.5 μmol N L^{-1}, 7.5 ± 0.8‰, and −2.5 ± 0.5 μmol N L^{-1} in E-AAIW, respectively; 43.0 ± 0.6 μmol N L^{-1}, 6.6 ± 1.1‰, and
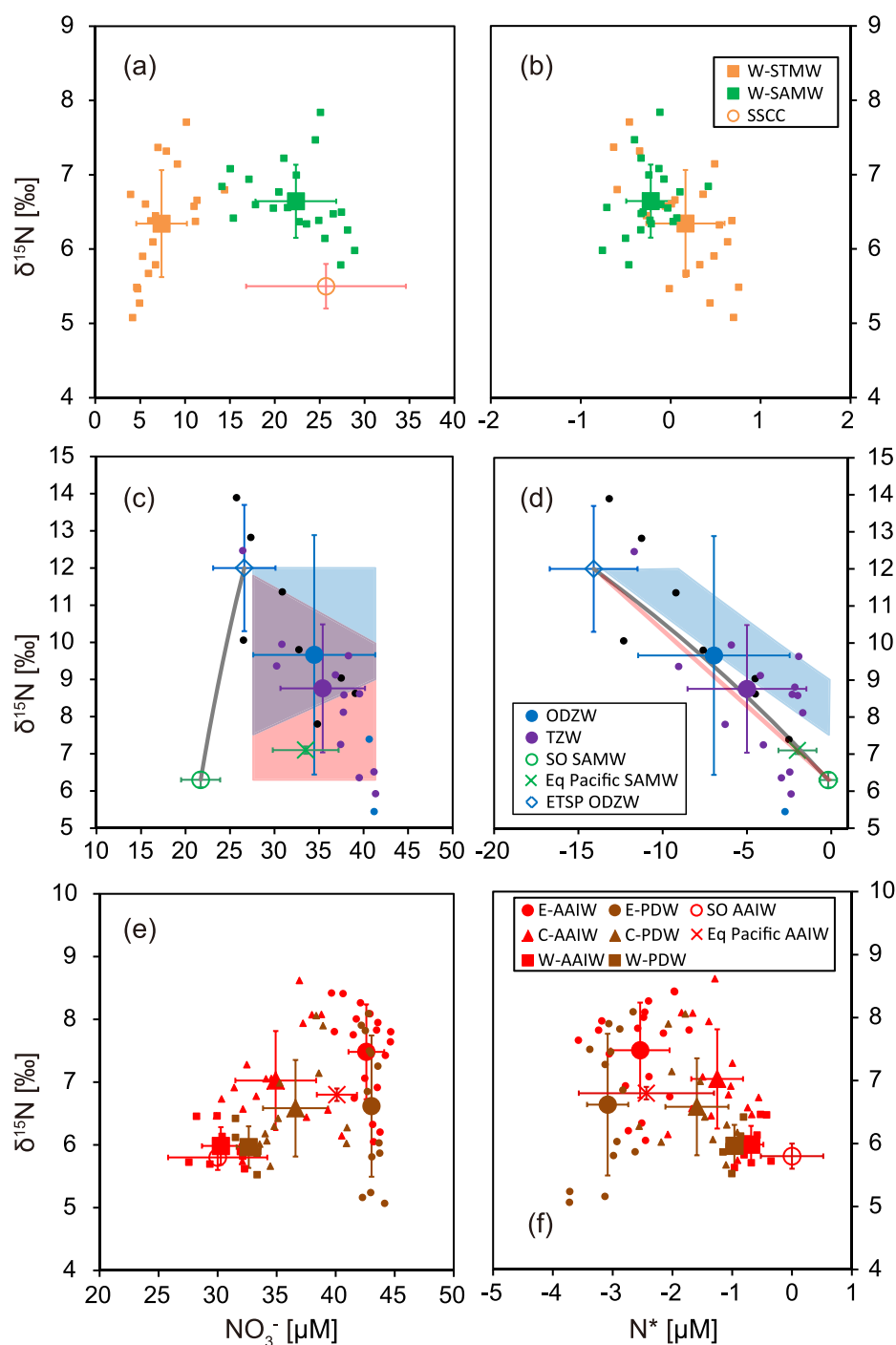
Figure 5. The relationship between NO_3^- concentrations (μmol N L^{-1}) and δ^{15}N–NO_3^- values (‰), and the relationship between N* values (μmol N L^{-1}) and δ^{15}N–NO_3^- values (‰) in (a and b) western surface and subsurface waters, (c and d) eastern intermediate waters, and (e and f) deep waters. Gray lines in Figures 5c and 5d represent mixing lines between SO SAMW and ETSP ODZW. Red and blue shaded areas denote cases in which organic matter remineralizes with values of N* = 0 and δ^{15}N–NO_3^- = 6.3‰, and N* = 0 and δ^{15}N–NO_3^- = 12.0‰, respectively, and the purple shaded area denotes both cases. The remineralized NO_3^- concentrations are between 6 and 20 μmol N L^{-1}. Small and large closed symbols show observed values and averaged values of each water mass, respectively. Black dots show samples in which oxygen concentrations are less than 15 μmol kg^{-1}. Large open symbols show averaged values observed by previous studies as follows. The Eq. Pacific SAMW and SSCC values are referenced from *Rafter et al.* [2012]. The SO SAMW values are from *Sigman et al.* [2000]. The ETSP ODZW values are from *Liu* [1979] and *De Pol-Holz et al.* [2009].

-3.1 ± 0.3 μmol N L^{-1} in E-PDW, respectively) than SO AAIW (30.0 ± 4.2 μmol N L^{-1}, $5.8 \pm 0.3\permil$, and 0.0 ± 0.6 μmol N L^{-1}, respectively) (Figures 5e and 5f). These results indicate that E-AAIW and E-PDW are affected by mixing with denitrified water with negative N* values and high δ^{15}N–NO$_3^-$ values, as well as by the remineralization of organic matter. AAIW in the equatorial Pacific has much higher NO$_3^-$ concentrations and δ^{15}N–NO$_3^-$ values and much lower N* values (40.1 ± 1.7 μmol N L^{-1}, $6.8 \pm 0.3\permil$ and -2.4 ± 1.3 μmol N L^{-1}, respectively) than does SO AAIW, and has slightly lower NO$_3^-$ concentrations and δ^{15}N–NO$_3^-$ values, and slightly higher N* values than does E-AAIW (42.6 ± 1.5 μmol N L^{-1}, $7.5 \pm 0.8\permil$ and -2.5 ± 0.5 μmol N L^{-1}, respectively). These results show that during transport from the Southern Ocean to the subtropical South Pacific, AAIW is affected by mixing with denitrified water with negative N* and high δ^{15}N–NO$_3^-$ values. The negative N* and high δ^{15}N–NO$_3^-$ signals are then diluted as the water mass is transported from the subtropical South Pacific to the equatorial Pacific.

4. Conclusion

The δ^{15}N values of NO$_3^-$ (δ^{15}N–NO$_3^-$) transfer to the δ^{15}N values of phytoplankton, settling particles, and eventually benthic sediment, whereas the levels of N* do not transfer. The δ^{15}N value of sediments can therefore be used to trace the past nitrogenous nutrient environment. In our study, the subsurface waters between 160°E and 170°W were affected by N fixation, with samples showing relatively low δ^{15}N–NO$_3^-$ values. Moreover, the subsurface waters east of 115°W were affected by denitrification, with samples showing relatively high δ^{15}N–NO$_3^-$ values. The δ^{15}N values of sediments in the subtropical South Pacific are therefore expected to reveal past changes in N fixation or denitrification in the subtropical South Pacific.

De Pol-Holz et al. [2009] confirmed the transfer of enriched-δ^{15}N values generated by water column denitrification from NO$_3^-$ to the sediment in the eastern South Pacific. Furthermore, *De Pol-Holz et al.* [2007] reconstructed changes in N removal by water column denitrification in the eastern South Pacific during the last 70,000 years. In our study, water column denitrification is recorded in the δ^{15}N–NO$_3^-$ values of subsurface waters in the eastern South Pacific. The N fixation activities and *Trichodesmium* abundances have also been detected in and near our study area [*Moutin et al.*, 2008]. The δ^{15}N value of the sediment is lower when denitrification occurs at the same time and place as N fixation than that when only denitrification occurs. Therefore, we conclude that both denitrification and N fixation are recorded in the δ^{15}N–NO$_3^-$ value and that the magnitude of denitrification is likely to be underestimated. The δ^{15}N–NO$_3^-$ values reflect the outcomes of various biogeochemical processes as well as water circulation. The reconstruction of N fixation and denitrification separately and quantitatively using δ^{15}N values of porphyrins as molecular markers of chlorophyll families in sediment [e.g., *Kashiyama et al.*, 2008], as well as the measurement of δ^{15}N values of organic N bound within diatoms [e.g., *Robinson et al.*, 2004] and the development of a marine N isotope model coupled with physical processes [e.g., *Yoshikawa et al.*, 2005] are expected to provide a more precise understanding of the past nitrogenous nutrient environment in the subtropical South Pacific.

References

Barford, C. C., J. P. Montoya, M. A. Altabet, and R. Mitchell (1999), Steady-state nitrogen isotope effects of N$_2$ and N$_2$O production in *Paracoccus denitrificans*, *Appl. Environ. Microbiol.*, 65, 989–994.

Casciotti, K. L., and M. R. McIlvin (2007), Isotopic analyses of nitrate and nitrite from reference mixtures and application to eastern tropical North Pacific waters, *Mar. Chem.*, 107, 184–201, doi:10.1016/j.marchem.2007.06.021.

Clark, L. L., E. D. Ingall, and R. Benner (1998), Marine phosphorus is selectively remineralized, *Nature*, 393, 426.

De Pol-Holz, R., O. Ulloa, F. Lamy, L. Dezileau, P. Sabatier, and D. Hebbeln (2007), Late Quaternary variability of sedimentary nitrogen isotopes in the eastern South Pacific Ocean, *Paleoceanography*, 22, PA2207, doi:10.1029/2006PA001308.

De Pol-Holz, R., R. S. Robinson, D. Hebbeln, D. M. Sigman, and O. Ulloa (2009), Controls on sedimentary nitrogen isotopes along the Chile margin, *Deep Sea Res., Part II*, 56, 1042–1054.

Deutsch, C., N. Gruber, R. M. Key, J. L. Sarmiento, and A. Ganachaud (2001), Denitrification and N$_2$ fixation in the Pacific Ocean, *Global Biogeochem. Cycles*, 15(2), 483–506, doi:10.1029/2000GB001291.

Elliott, E. M., C. Kendall, E. W. Boyer, D. A. Burns, G. G. Lear, H. E. Golden, K. Harlin, A. Bytnerowicz, T. J. Butler, and R. Glatz (2009), Dual nitrate isotopes in dry deposition: Utility for partitioning NO$_x$ source contributions to landscape nitrogen deposition, *J. Geophys. Res.*, 114, G04020, doi:10.1029/2008JG000889.

Granger, J., D. M. Sigman, M. F. Lehmann, and P. D. Tortell (2008), Nitrogen and oxygen isotope fractionation during dissimilatory nitrate reduction by denitrifying bacteria, *Limnol. Oceanogr. Methods*, 53(6), 2533–2545.

Großkopf, T., W. Mohr, T. Baustian, H. Schunck, D. Gill, M. M. M. Kuypers, G. Lavik, R. A. Schmitz, D. W. R. Wallace, and J. LaRoche (2012), Doubling of marine dinitrogen-fixation rates based on direct measurements, *Nature*, 488(7411), 361–364.

Gruber, N., and J. L. Sarmiento (1997), Global patterns of marine nitrogen fixation and denitrification, *Global Biogeochem. Cycles*, 11(2), 235–266.

Johnson, G. C., and K. E. McTaggart (2010), Equatorial Pacific 13°C water eddies in the eastern subtropical South Pacific Ocean, *J. Phys. Oceanogr.*, *40*, 226–236, doi:10.1175/2009 JPO4287.1.

Kashiyama, Y., N. O. Ogawa, M. Shiro, R. Tada, H. Kitazato, and N. Ohkouchi (2008), Reconstruction of the biogeochemistry and ecology of photoautotrophs based on the nitrogen and carbon isotopic compositions of vanadyl porphyrins from Miocene siliceous sediments, *Biogeosciences*, *5*, 797–816, doi:10.5194/bg-5-797-2008.

Kritee, K., D. M. Sigman, J. Granger, B. B. Ward, A. Jayakumar, and C. Deutsch (2012), Reduced isotope fractionation by denitrification under conditions relevant to the ocean, *Geochim. Cosmochim. Acta*, *92*, 243–259.

Liu, K. K. (1979), Geochemistry of inorganic nitrogen compounds in two marine environments: The Santa Barbara Basin and the ocean off Peru, PhD thesis, Univ. of South. Calif., Los Angeles, Calif.

Martiny, A. C., C. T. A. Pham, F. W. Primeau, J. A. Vrugt, J. K. Moore, S. A. Levin, and M. W. Lomas (2013), Strong latitudinal patterns in the elemental ratios of marine plankton and organic matter, *Nat. Geol.*, *6*, 279–283.

Minagawa, M., and E. Wada (1986), Nitrogen isotope ratio of red tide organisms in the East China Sea: A characterization of biological nitrogen fixation, *Mar. Chem.*, *19*, 245–259.

Miyake, Y., and E. Wada (1971), The isotope effect on the nitrogen in biochemical, oxidation-reduction reactions, *Rec. Oceanogr. Works Jpn.*, *11*, 1–6.

Mohr, W., T. Grosskopf, D. W. R. Wallace, and J. LaRoche (2010), Methodological underestimation of oceanic nitrogen fixation rates, *PLoS One*, *5*, e12583, doi:10.1371/journal.pone.0012583.

Moutin, T., D. M. Karl, S. Duhamel, P. Rimmelin, P. Raimbault, B. A. S. Van Mooy, and H. Claustre (2008), Phosphate availability and the ultimate control of new nitrogen input by nitrogen fixation in the tropical Pacific Ocean, *Biogeosciences*, *5*, 95–109.

Naqvi, S. W. A., M. Voss, and J. P. Montoya (2008), Recent advances in the biogeochemistry of nitrogen in the ocean, *Biogeosciences*, *5*, 1033–1041.

Pierotti, D., and R. A. Rasmussen (1980), Nitrous oxide measurements in the eastern tropical Pacific Ocean, *Tellus*, *32*(1), 56–72.

Rafter, P. A., D. M. Sigman, C. D. Charles, J. Kaiser, and G. H. Haug (2012), Subsurface tropical Pacific nitrogen isotopic composition of nitrate: Biogeochemical signals and their transport, *Global Biogeochem. Cycles*, *26*, GB1003, doi:10.1029/2010GB003979.

Rafter, P. A., P. J. DiFiore, and D. M. Sigman (2013), Coupled nitrate nitrogen and oxygen isotopes and organic matter remineralization in the Southern and Pacific Oceans, *J. Geophys. Res. Oceans*, *118*, 4781–4794, doi:10.1002/jgrc.20316.

Redfield, A. C., B. H. Ketchum, and F. A. Richard (1963), The influence of organisms on the composition of seawater, in *The Sea*, edited by M. N. Hill, pp. 27–77, Interscience, N. Y.

Robinson, R. S., B. G. Brunelle, and D. M. Sigman (2004), Revisiting nutrient utilization in the glacial Antarctic: Evidence from a new method for diatom-bound N isotopic analysis, *Paleoceanography*, *19*, PA3001, doi:10.1029/2003PA000996.

Savarino, J., S. Morin, D. M. Sigman, and M. H. Thiemens (2007), Nitrogen and oxygen isotopic constraints on the origin of atmospheric nitrate in coastal Antarctica, *Atmos. Chem. Phys.*, *7*(8), 1925–1945.

Shiozaki, T., T. Kodama, and K. Furuya (2014), Large-scale impact of the island mass effect through nitrogen fixation in the western South Pacific Ocean, *Geophys. Res. Lett.*, *41*, 2907–2913, doi:10.1002/2014GL059835.

Sigman, D. M., M. A. Altabet, D. C. McCorkle, R. Francois, and G. Fischer (2000), The δ^{15}N of nitrate in the Southern Ocean: Nitrogen cycling and circulation in the ocean interior, *J. Geophys. Res.*, *105*(C8), 19,599–19,614, doi:10.1029/2000JC000265.

Sigman, D. M., K. L. Casciotti, M. Andreani, C. Barford, M. Galanter, and J. K. Böhlke (2001), A bacterial method for the nitrogen isotopic analysis of nitrate in seawater and freshwater, *Anal. Chem.*, *73*(17), 4145–4153.

Sigman, D. M., P. J. DiFiore, M. P. Hain, C. Deutsch, Y. Wang, D. M. Karl, A. N. Knapp, M. F. Lehmann, and S. Pantoja (2009), The dual isotopes of deep nitrate as a constraint on the cycle and budget of oceanic fixed nitrogen, *Deep Sea Res., Part I*, *56*, 1419–1439, doi:10.1016/j.dsr.2009.04.007.

Yoshikawa, C., Y. Yamanaka, and T. Nakatsuka (2005), An ecosystem model including nitrogen isotopes: Perspectives on a study of the marine nitrogen cycle, *J. Oceanogr.*, *61*, 921–942.

Yoshikawa, C., V. J. Coles, R. R. Hood, D. G. Capone, and N. Yoshida (2013), Modeling how surface nitrogen fixation influences subsurface nutrient patterns in the North Atlantic, *J. Geophys. Res. Oceans*, *118*, 2520–2534, doi:10.1002/jgrc.20165.